Proceedings of the International Association for Shell and Spatial Structures (IASS) Symposium 2009, Valencia
Evolution and Trends in Design, Analysis and Construction of Shell and Spatial Structures
28 September – 2 October 2009, Universidad Politecnica de Valencia, Spain
Alberto DOMINGO and Carlos LAZARO (eds.)

Influence of patch-load on metal silos with corrugated walls

Francisco AYUGA*, Carlos GONZALEZ-MONTELLANO [a], Eutiquio GALLEGO[b], José María FUENTES[a] Álvaro RAMIREZ[c]

[*a] ETSI Agrónomos, Universidad Politécnica de Madrid,
Ciudad Universitaria S/N 28040 Madrid (Spain), Bipree Research Group
francisco.ayuga@upm.es

[b]EUIT Agrícola, Universidad Politécnica de Madrid (Spain)
[c]EUIT Industrial, Universidad Politécnica de Madrid (Spain)

Abstract

Silos are widely used in food industries to store different types of agricultural products. Loads exerted by the stored material on silo walls are critical in the design of the shell structure. Eurocode standard represents these loads by means of symmetrical pressure distributions and unsymmetrical pressure distributions, this latter named patch-load. In this paper, the structural effects of the patch load are investigated. A 3D FEM model has been developed to model cylindrical flat bottom silos made of corrugated steel walls. Firstly, silos were modelled only with the effect of the symmetrical pressure distributions. The structural effects at this stage were compared to those obtained in a second stage, where the patch-load was introduced in the model. The purpose of this research work was to understand the structural effects of the patch-load as described in the Eurocode, as well as validate analytical expressions to determine these effects more easily.

Keywords: Silo, patch-load, steel silos, corrugated walls, FEM.

1. Introduction

Part 4 of Eurocode 1 (EN 1991-4 (2006) [5]) is often the benchmark regulation within the European area for the determination of the actions exerted by the material stored inside the silos. These actions are represented by pressure distributions on the silo wall, for both filling and discharge situations of the silo, and may be symmetric and global or asymmetric and local. The mission of these latter distributions is to take account of possible load asymmetries due to eccentricities and/or imperfections present in the charging and discharging process (Gille and Rotter, 2002 [6], Song and Teng, 2003 [11]).

Symmetric distributions comprise both horizontal pressures (P_h) and friction pressures (P_w), applied on all points of the silo wall in contact with the material stored and present axial symmetry, albeit with pressure values that increase with depth. On the other hand, local

asymmetric distributions (patch load) comprise only horizontal pressures and their application area is restricted to a localized strip of wall, and this strip may be located at any depth z_p of the silo (Figure 1). The pressure values characterizing it (P_{ps}) are constant for a single meridional line of the strip but there is a continuous variation with the circumferential co-ordinate Θ (they do not present axial symmetry).

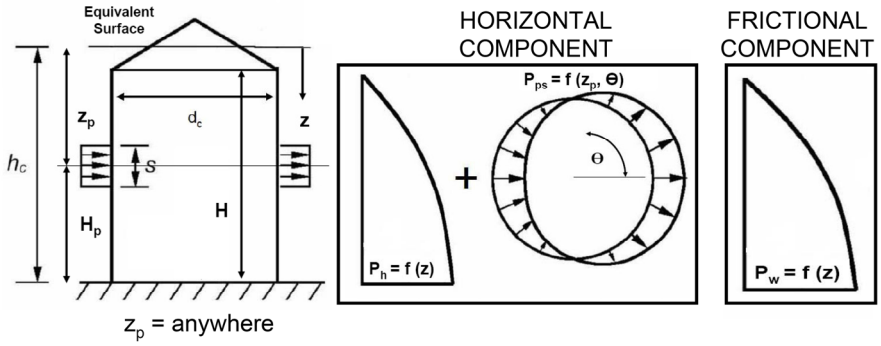

Figure 1. Distributions of pressures representing the action of the material stored.

The structural effects derived from symmetric pressure distributions are easy to calculate using classical analytical expressions (Janssen 1895 [7], Reimbert&Reimbert 1959 [8]). Nonetheless, the determination of the effects produced by asymmetric distribution is not so immediate (Ayuga, 2008 [2], Song, 2003 [10], Brown and Nielsen, 1998 [4]), because of both its asymmetric nature and its arbitrary position. As a result, the EN 1991-4 [5] standard in certain cases allows consideration of the patch load to be ignored or simplified. However, its consideration must be strict in the case of large-scale silos, where it is very common to use corrugated steel sheets on the silo wall.

The literature contains several papers on the effects of patch load (Briassoulis, 2000 [3], Gille and Rotter, 2002 [6], Song and Teng, 2003 [11]) as well as analytical procedures for estimating the effects of patch load (Rotter, 2001 [9]), but they mainly focus on smooth wall silos. For other cases, it would be necessary to resort to numerical methods, such as MEF, for the study of their effects.

The purpose of the present paper is to investigate the structural effects due to patch load on cylindrical silos with walls made of corrugated steel. Through an understanding of these, it will be possible to validate new or pre-existing analytical procedures that facilitate strict consideration of the patch load.

2. Methodology

In order to achieve the goals indicated, MEF has been used to analyze an extensive series of silos (S) in which the patch load has to be considered strictly. The overall geometry of these silos, characterized by the diameter d_c and height H of their cylindrical body, is that indicated in Table 1, with the local geometry (corrugation) of the walls as represented in Figure 2. Although the real local geometry to be simulated is corrugated, it has been

considered to be made up of different straight segments because, on the one hand, this facilitates the application of loads in the model and, on the other, the fact that the generation of a mesh of finite elements on a curved element implies the subsequent discretization of the curvature in small straight segments.

The stored material in the silo is considered to be wheat and its effects will be simulated directly based on the thrust values produced on the silo wall. Specifically, each case will be analyzed solely under the loads associated with the horizontal pressure component (Figure 1), comprising a symmetric distribution and an asymmetric distribution of horizontal pressures. To be able to appreciate the effects due to the presence of the patch load, two different load states (T) are established. The first load state (T1) will only consider a symmetric pressure distribution, whereas the second load state (T2) will consider both symmetric and asymmetric local distribution.

Load state T2 involves asymmetric pressure distribution, which may be located at any position within the silo, as per EN 1991-4 [5]. In order to take this situation into account, consideration will be given to four possible positions of the patch load for each of the silos S indicated in Table 1. Where H_p is the generic distance between the centre of the strip where the patch load is applied and the base of the silo, the four discrete patch load positions (P) will be those associated with the values of H_p for H/5 (P1), 2H/5 (P2), 3H/5 (P3) and 4H/5 (P4).

Silo (S)	d_c (m)	H (m)	λ (h_c/d_c)	Capacity (t)
S1	21.83	29.28	1.34	10062.8
S2	21.83	30.39	1.39	10447.0
S3	21.83	31.51	1.44	10831.1
S4	23.65	25.01	1.06	10089.0
S5	23.65	26.13	1.10	10539.8
S6	23.65	27.25	1.15	10990.7
S7	23.65	28.36	1.20	11441.5
S8	23.65	29.48	1.25	11892.3
S9	23.65	30.60	1.29	12343.2
S10	23.65	31.72	1.34	12794.0
S11	27.29	27.65	1.01	14852.2
S12	27.29	28.77	1.05	15452.4
S13	27.29	29.89	1.10	16052.6
S14	27.29	31.00	1.14	16652.8
S15	27.29	32.12	1.18	17253.1
S16	27.29	32.64	1.02	23857.1

$$h_c = H + \frac{d_c}{6}\tan\phi_r \qquad (\text{Ø}_r \text{ Rest angle of the stored material})$$

Table 1. Geometric characteristics of the silos

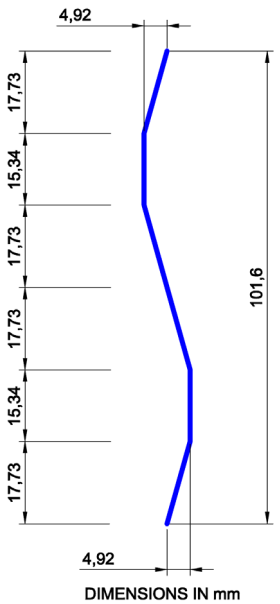

Figure 2. Geometry of the wall corrugation.

The pressure values of the horizontal component (for both symmetric and asymmetric distribution) have been determined in accordance with the procedures established in EN

1991-4 [5], considering in all cases that the silo was under discharge. The characteristic parameters of the material stored (wheat) will be those given in Appendix E of the EN 1991-4 [5] standard.

All cases will be simulated by considering different wall thicknesses along its height, a common occurrence in reality, as it allows adaptation of the wall's resistance at the level of the pressures received at each point. The thicknesses considered in the cases analyzed in the present paper have been determined by preliminary analytical calculations based solely on the values of the symmetric pressure distributions. In order to take into account in some way the influence of the patch load on the value of these thicknesses, the values of these symmetric distributions have been increased for patch load reasons in accordance with the simplified procedure established in EN 1991-4 (5.2.3) [5].

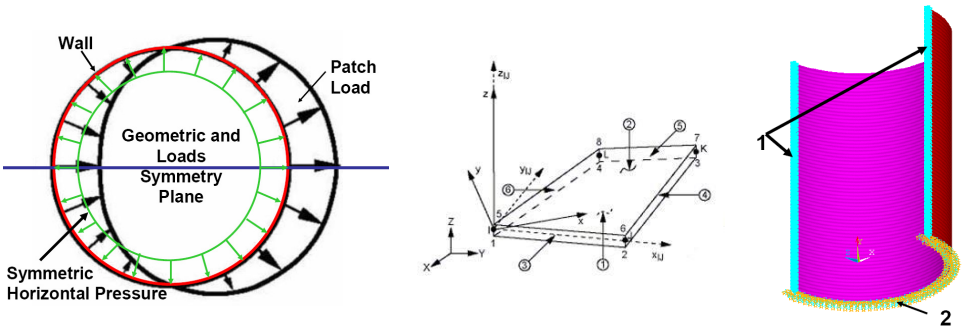

(a) (b) (c)

Figure 3. Characteristics of the finite element model.

The finite element model developed only simulates one of the symmetric halves of the silo wall (Figure **3** (a)) and its mesh has been realized using the SHELL 63 element in the library of the ANSYS commercial programme [1]. This element is a flat-plane quadrilateral element capable of simulating flexion and membrane effects. The element (Figure **3** (b)) has four nodes distributed on the four corners of the element, with potentially six degrees of freedom per node. The behaviour of the material simulated by the element will be an elastic, linear and isotropic model defined through the elasticity modulus and the Poisson coefficient characterizing steel (E = 210,000,000 kPa and υ = 0.3).

In order to achieve equilibrium in the resolution of the model and consider the influence of the unsimulated symmetric half, certain constraints have been established for some nodes in the model. The nodes located on the base of the silo (Figure **3** (c) – 2 –) have all their rotations and displacements prevented, whereas the nodes located on the extreme vertical lines of the model (Figure **3** (c) – 1 –) have circumferential displacement constrained.

3. Results.

All cases S in Table 1 have been analyzed in both load states (T) indicated, considering for load state T2 the four positions P of the patch load stipulated in Part 2. Additionally,

consideration has been given to five generatrices (L) uniformly distributed in the half of the silo modelled (Figure 4).

Figure 4. Position of the generatrices L

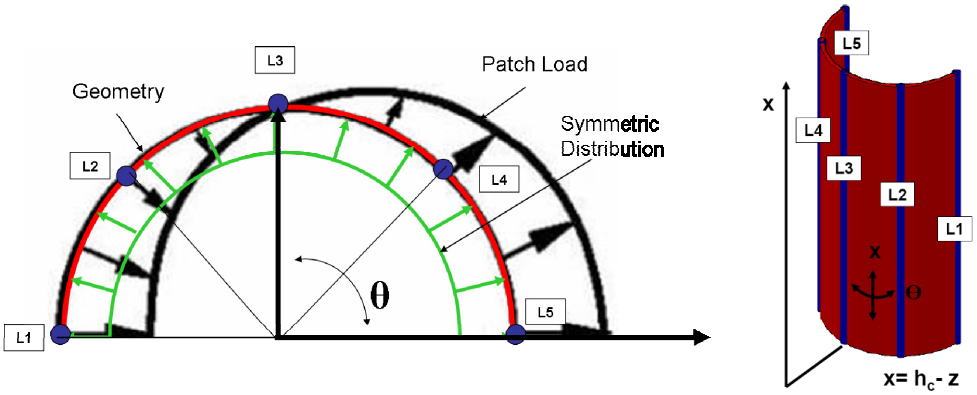

For any combination S-T-P-L, curves have been extracted to show the evolution of the stress resultant values (R) on the wall with the meridional co-ordinate x (Figure 4) of the generatrix L considered. Generically, these curves will be expressed as:

$$R = f(x, S, T, P, L) \tag{1}$$

This function will always be represented bidimensionally (R = f(x)) for pre-set values of the variables S, T, P and L. The stress resultants R obtained are as indicated in Figure 5 and are considered to be expressed per unit of length.

Figure 5. Stress resultants considered on the silo wall (positive values)

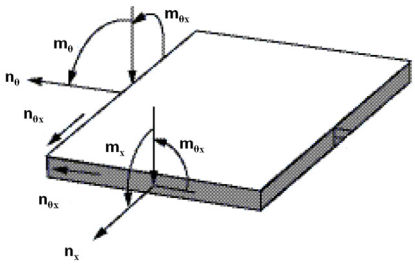

In load state T1, the stress resultant curves obtained for any line L are qualitatively and quantitatively identical due to the axial symmetric character of the geometry and the pressure distribution in this state.

After analyzing the stress resultant curves of all the possible combinations in load state T2, it was seen that, for a given generatrix L, the results of any combination S – P are

qualitatively equal. It was also seen that the most unfavourable effects of the patch load are due to normal stresses in the circumferential and meridional directions on the extreme generatrices of the model (L1 and L5). In the case of the intermediate generatrices, the effects detected for lines L2 and L4 are qualitatively equal but quantitatively of less intensity than those obtained, respectively, for L1 and L5 lines. In the case of generatrix L3, due to the fact that its position coincides with the point of the distribution of the patch load at which the pressures become zero, the results obtained do not differ from those presented for state T1.

Due to the above, the illustration in Figure 6 shows an example of the axial meridional curves (n_x), axial circumferential curves (n_Θ), meridional moment (m_x) and circumferential moment (m_Θ) for case S3. Figure 6 – a) shows the results of load state T1 for any generatrix L (note that T1 only involves symmetric loads, so all the lines L present the same stress values). Figure 6 – b) and Figure 6 – c) show the results of load state T2 with a position of patch load P4 and for the extreme generatrices L5 and L1.

3.1 Circumferential membrane stress resultant (n_θ).

The curve of n_θ in Figure 6 – a) coincides with the effect expected in the structure in load state T1, which only has symmetric distribution. This effect is that of a circumferential traction of uniform value for a single height z and proportional to that of the horizontal pressure at that height, with the proportionality constant being the radius of the silo (r_c):

$$n_\theta(z) = p_h(z) \cdot r_c \tag{2}$$

In load state T2, there are modifications in the circumferential membrane stress resultants due to the addition of the patch load distribution on the silo. These modifications only occur locally on the strip where the patch load is applied and provoke an increase in the value of the circumferential traction resultant on L5 and a reduction on L1.

The foregoing is due to the patch load distribution generating circumferential traction or compression stresses, respectively, in those positions where this distribution presents outward or inward pressures in the silo. In addition, this traction or compression is greater the greater the outward or inward pressure, where this variation depends on the angle Θ associated with the point considered.

These observations can be explained analytically as follows: for a patch load located at a depth z_p with respect to the equivalent surface (Figure 1) and for a circumferential co-ordinate point Θ (Figure 4) located inside the strip for application of the load, the (positive) traction or (negative) compression value will be given by the following analytical expression:

$$n_\theta = P_{ps}(z_p, \theta) \cdot r_c \tag{3}$$

Figure 6. Wall stress resultant curves for case 3C4 in load states T1 and T2.

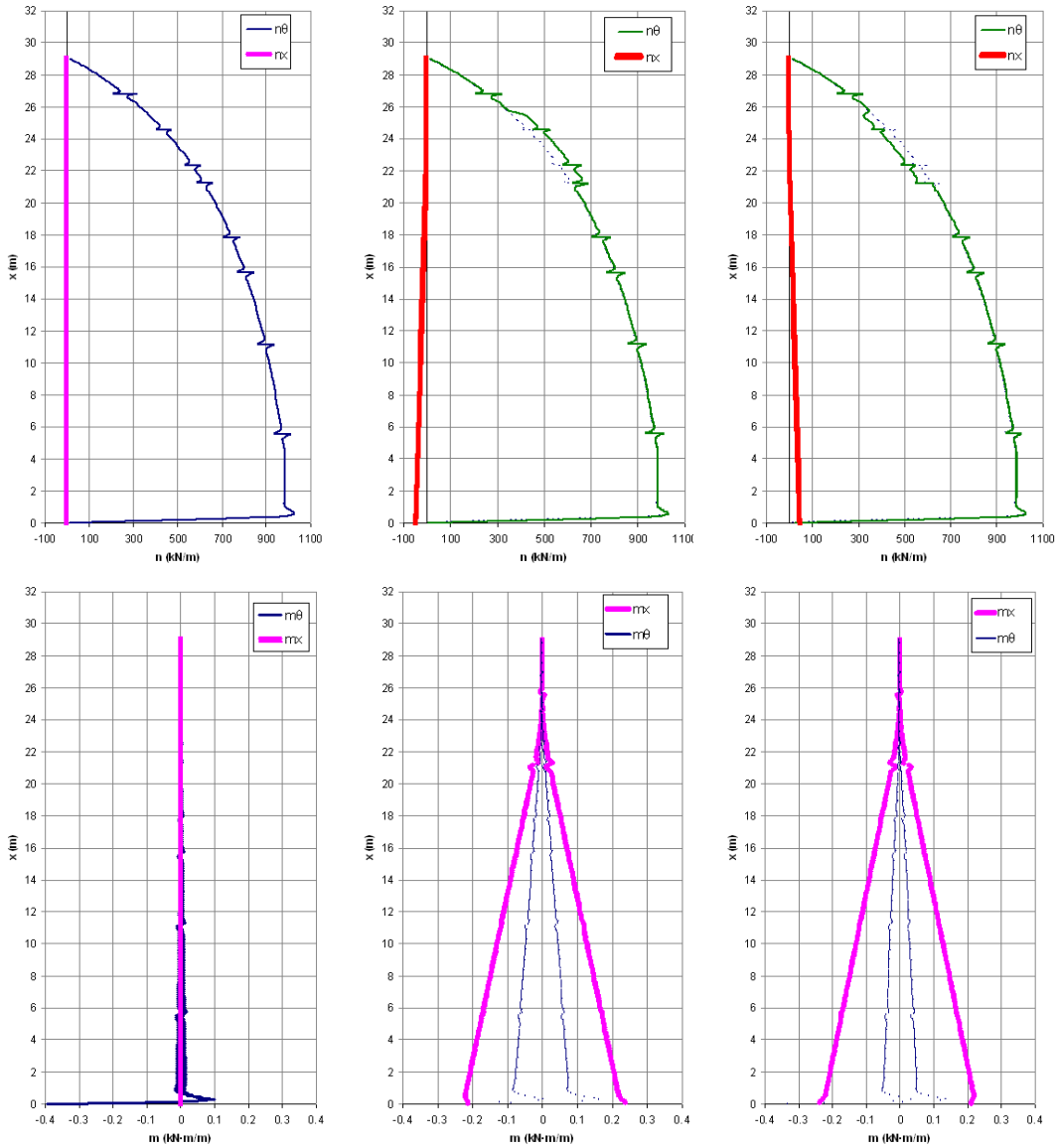

a) S3 T1 b) S3 T2 C4 L5 c) S3 T2 C4 L1

The value of P_{ps} as defined in standard EN 1991-4 [5] (Figure 1) depends on the value of the horizontal pressure P_h of the symmetric component at height z_p where the patch load is

considered to be applied and the circumferential co-ordinate Θ of the point considered through the cosine of this angle:

$$P_{ps}(z_p,\theta) = C_p \cdot P_h(z_p) \cdot \cos(\theta) \tag{4}$$

Since the value of P_h increases with depth, the value of n_Θ will be greater, for a given circumferential co-ordinate, at deeper patch load positions. For a specific position of the patch load (fixed z_p), the value of n_Θ varies between a maximum traction value at $\Theta = 0º$ and a maximum compression value at $\Theta = 180º$, passing through a zero value at $\Theta = 90º$.

The expression resulting from the combination of (3) and (4) coincides with that given by Rotter [9] for the case of smooth-walled silos.

3.2. Meridional membrane stress resultant (n_x).

In load state T1, the development of n_θ is sufficient to balance the symmetric pressure distribution, so there are no meridional membrane stress resultants recorded in this state. However, the patch load considered in load state T2 implies the existence of a pressure distribution with a certain resultant force. This resultant force is the force F applied at a depth z_p (position in the centre of the strip to which the patch load is applied, Figure 1) and oriented in the same sense as pressures in this distribution. Its value comes from integrating equation [4] throughout the perimeter of the silo and for the height strip to which the patch load is applied:

$$F(z_p) = 0{,}5 \cdot \pi \cdot d_c C_p \cdot P_h(z_p) \tag{5}$$

This point force is responsible for the emergence of a moment with value $M = F\,(z\text{-}z_p)$ (Figure 7) in a transverse section of the silo located at a depth z (Figure 1) below the point where the patch load is applied.

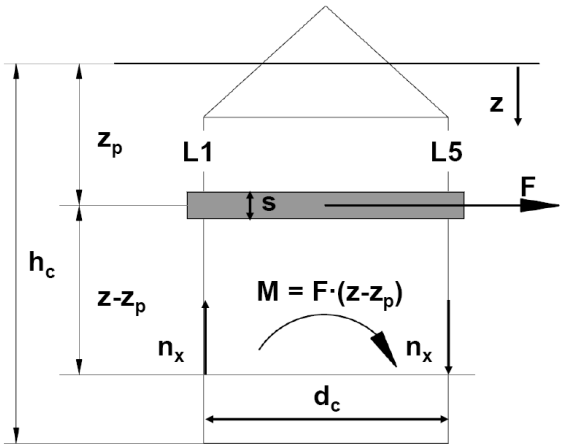

Figure 7. Diagram for the analytical determination of n_x

This moment would be offset by normal compression and traction stresses on either side of the flexion axis (in this case the flexion axis would be formed by the line joining the centre of the silo with the zero pressure points of the patch load distribution). In addition, these compression and traction forces would be equal, in absolute terms, at points on the silo wall located symmetrically to the flexion axis.

All of the above coincides with the results observed in the diagram of n_x in Figure 6 – b) and Figure 6 – c) for the generatrices L1 and L5 in load state T2. These generatrices are located at those points furthest from the flexion axis and, in addition, symmetrically to it. This means that the values of n_x for both generatrices (traction (L1) and compression (L5)) are the maximum possible, and are also equal in absolute values. This absolute value increases linearly from the point of application of the patch load to the base of the silo and the cause of this linearity is the factor $(z - z_p)$ of the expression of M (the force F remains constant for a given position of the patch load).

The value of n_x for a point on the wall with co-ordinates (z, Θ) due to a patch load located at a depth z_p may be found analytically by simply performing the study of a particular transverse section of the silo (located under the point where the patch load is applied) as if this section where that of a beam subjected to a bending moment M:

$$n_x(\theta, z, z_p) = -\frac{F(z - z_p)}{\frac{I}{0{,}5 \cdot d_c \cos(\theta)}} t \tag{6}$$

Where I is the inertia modulus of a circular ring with diameter d_c and t the thickness of the silo wall at the depth z under consideration. Replacing the value of I in expression [6] and combining it with expression [5] would give the following expression:

$$n_x(\theta, z, z_p) = -C_p \cdot P_h(z_p) s \frac{(z - z_p)}{0{,}5 \cdot d_c} \cos(\theta) \tag{7}$$

This expression coincides with that given by Rotter [9] for the case of smooth-wall silos.

For a given position of the patch load and a given vertical co-ordinate (fixed z_p and z), the value of n_x varies with the circumferential co-ordinate depending on its cosine value. This makes the value n_x take on negative (compression) values at points with $\Theta < 90º$, positive (traction) values with $\Theta > 90º$. The maximum absolute values of these compression or traction forces are, respectively, for $\Theta = 0º$ and $\Theta = 180º$, with the minimum zero value for the case of $\Theta = 90º$.

Given a position of the patch load and a single generatrix of the silo (where z_p and Θ are fixed), the value of n_x grows linearly with depth below the point at which the patch load is applied until it reaches a maximum value at the base of the silo.

For a specific point on the silo wall with co-ordinates (z, Θ), the value of n_x depends, on the one hand, on the pressure P_h at the height of the patch load position (z_p), which is greater the greater the depth at which this load is located. On the other hand, the value of n_x also depends on the factor $(z\text{-}z_p)$, which takes on greater values as the distance increases from

the patch load to the study point (generally when the patch load is located at a shallow depth z_p). This means that it is not possible to establish which patch load position generates the greatest value for n_x at a particular point (z, Θ) on the silo, and this position may also change when the point under study is different.

3.3. Bending moments m_x

As in the case of n_x, no moments m_x are developed during load state T1, as the horizontal symmetric pressures in this state are only balanced by the development of circumferential forces. Nonetheless, in load state T2 moments m_x appear at all points lying below the point where the patch load is applied, and it gradually and linearly increases with depth.

The evolution of m_x is analogous and proportional to that described for n_x, suggesting that both must be related through some proportionality constant. This proportionality constant is found by assuming that the vertical stress resultant n_x flows down the mid-plane of the wall, a distance b away from the vertical plane stretches of the corrugation geometry (Figure 8). This situation leads to the appearance of m_x moments, which could be analytically determined by:

$$m_x = n_x \cdot b \tag{8}$$

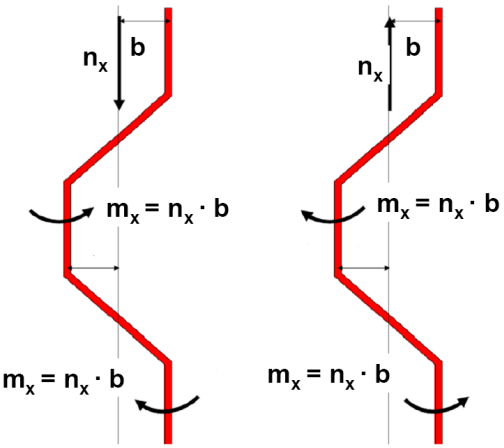

Figure 8. Justification of the appearance of moment m_x as a consequence of the axial n_x

The final sign of the m_x moment depends on the sign of n_x (traction or compression) and on the sign of the distance b (indicating whether the vertical plane element considered lies inward or outward from the mid-plane of the wall). This variation in the sign of m_x with the sign of the distance b is the cause of the double branch characteristic of the m_x curve (Figure 6) for a single generatrix L.

As can be seen, the emergence of m_x is a consequence of the wall's corrugated geometry and this moment does not exist in the case of smooth-walled silos.

3.4. Bending moments m_Θ

The behaviour of the circumferential bending moments (m_θ) is similar to that described for the case of m_x, although in this case their presence is due to the ovalization of the cross section of the silo in positions below the point where the patch load is applied.

Nonetheless, for designing purposes, the stresses deriving from m_θ will have no relevance. This is due to the fact that the design of the silo must guarantee sufficient resistance against any possible location of the patch load and, for a patch load position i, the circumferential stresses due to m_θ at points below where it is applied are less than the circumferential stresses present in the strip where a patch load j is applied, with a lower application point than patch load i. The stresses due to this moment are relevant for patch load strips in high positions of the silo but in that case are lower than those produced by the patch load on strips located in low positions and, as these cannot be superimposed, this second situation will predominate.

4. Conclusions

In the present paper, MEF has been used to study the structural effects of patch load, as defined in EC 1 - 4 [5], in cylindrical silos with walls made from corrugated sheets. The most unfavourable effects occur in two diametrically opposed generatrices located at the points where the pressure distribution of the patch load acquires max pressure values. These effects comprise:

- An axial circumferential (n_θ) on the strip where the patch load is applied, which may be traction or compression depending on the circumferential co-ordinate.
- An axial meridional (n_x) on points in the wall below the patch load. This is a consequence of the global moment acting on the silo cross-section in these positions and the non-zero resultant force of the patch load distribution. This axial may be traction or compression depending on the circumferential co-ordinate considered, with an absolute value that increases linearly with depth.
- A meridional moment (m_x) at points on the wall below the patch load. This is a consequence of the global eccentricity that exists between the axial meridional n_x and the position of the straight vertical stretches of the wall's corrugated geometry.
- A meridional moment (m_θ) at points on the wall below the patch load. This is a consequence of the ovalization of the cross-section of the silo at positions below the point where the patch load is applied. The stresses derived from this moment are not considered in the design of the silo.

By understanding these effects, it has been possible to validate analytical expressions allowing easier determination of the structural effects produced by the patch load. Of the analytical expressions provided, those corresponding to n_x and n_Θ coincide with those given in Rotter, 2001 [9] for the case of smooth sheet silos. That given for the case of m_x is exclusive to silos with corrugated sheets.

The goodness of fit between these expressions and the results obtained numerically is practically absolute, so the use of these analytical expressions is completely valid for determining the stress status at all points on the silo wall.

References

[1] ANSYS Users' Manual. ANSYS 10.0.

[2] Ayuga, F. (2008). Some unresolved problems in the design of steel cylindrical silos. In Structures and Granular Solids. From Scientific Principles to Engineering Applications. J F Chen, J Y Ooi and J G Teng editors. Ed. Taylor & Francis Group. London.

[3] Briassoulis, D. (2000), 'Finite element analysis of a cylindrical silo shell under unsymmetrical pressure distributions', *Computers & Structures* 78(1-3), 271-281.

[4] Brown C.J and Nielsen J. (1998) "Silos". E & FN Spon. London.

[5] EN 1991 – 4 (2006). Actions on structures. Silos and tanks.

[6] Gillie, M. & Rotter, J. M. (2002), 'The effects of patch loads on thin-walled steel silos', *Thin-Walled Structures* 40(10), 835-852.

[7] Janssen, H A. 1895. Versuche über getreidedruck in silozellen, Z. Ver. Dtsch. Ing. 39: 1045-1049.

[8] Reimbert A, Reimbert M. 1959. Silos, théorie et pratique. Editions Eyrolles, France

[9] Rotter, J.M. (2001). "Guide for the economic design of circular metal silos". Spon Press. London

[10] Song, C. Y. (2004), 'Effects of patch loads on structural behavior of circular flat-bottomed steel silos', *Thin-Walled Structures* 42(11), 1519-1542.

[11] Song, C. Y., Teng, J.G. (2003), 'Buckling of circular steel silos subject to code-specified eccentric discharge pressures', *Engineering Structures* 25, 1397-1417.